

Experimental:

1-Synthesis of Silver@Zinc Salen-MOF Composite

The synthesis process could be summarized as follows:

In the first step, zinc nitrate hexahydrate ($\text{Zn}(\text{NO}_3)_2 \cdot 6\text{H}_2\text{O}$, 2.0 mmol, 0.595 g) was completely dissolved in 10 mL of distilled water in a round-bottom flask. The organic nano-linker (1.0 mmol), previously prepared according to the method reported by *Sheta et al.*,³² was added to the flask. The zinc salt solution was then added dropwise to the organic linker suspension with continuous magnetic stirring for 30 minutes at room temperature. This step enabled the initial complexation of zinc ions with the organic linker, resulting in a helical complex through adduct formation at the nano-linker center skeleton. The resulting mixture was designated as Solution No. 1.

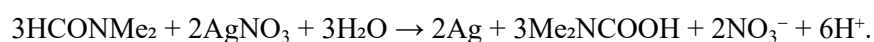
In the second step, silver nitrate (AgNO_3 , 2.0 mmol, 0.788 g) was dissolved separately in distilled water and then added dropwise to Solution No. 1 while maintaining continuous stirring for an additional 30 minutes. During this step, the silver ions underwent reduction by DMF, according to the proposed mechanism, and simultaneously incorporated into the outer nodes of the zinc-MOF structure through substrate binding. This process resulted in the formation of the final precursor solution designated as Solution No. 2.

The complete reaction mixture (Solution No. 2) was then transferred to a stainless-steel autoclave equipped with a Teflon lining to prevent contamination and ensure uniform heating. The autoclave was sealed and heated to 200°C for 8 hours under autogenous pressure to promote crystallization and proper framework formation. The hydrothermal conditions facilitated the complete coordination of metal ions with the organic linker, enabling the formation of a well-ordered MOF structure with incorporated silver nanoparticles.

After the hydrothermal treatment, the autoclave was allowed to cool naturally to room temperature. A fine light green-brown precipitate was observed, indicating successful formation of the Ag@Zn-SalenMOF composite. The precipitate was collected by filtration and washed thoroughly with distilled water to remove unreacted starting materials and by-products, followed by washing with ethanol to remove any organic impurities. The washed product was then dried under vacuum at 50°C for 24 hours to remove residual solvents and moisture. The final product was obtained as a light green-brown powder with a yield of 81.3% based on the theoretical molecular weight. The melting point of the synthesized composite was determined to be greater than 300°C, indicating high thermal stability. Elemental analysis of the final product showed good agreement with the calculated values for the proposed molecular formula $\text{C}_{42}\text{H}_{41}\text{Ag}_2\text{N}_9\text{O}_{12}\text{Zn}_2$ (molecular weight: 1210.34 g/mol). The calculated elemental composition was: C, 41.68%; H, 3.41%; Ag, 17.82%; N, 10.42%; O, 15.86%; Zn, 10.80%. The experimental values obtained from CHN analysis were: C, 40.92%; H, 3.52%; N, 10.39%, showing close agreement with the theoretical values and confirming successful synthesis of the target composite.

Proposed Reaction Mechanism

The synthesis mechanism involves two distinct steps that occur sequentially during hydrothermal. The first step involves the reduction of silver ions by DMF, which acts as a reducing agent under the reaction conditions. This reduction follows the chemical equation:



The use of DMF as a reducing agent for the synthesis of metal nanoparticles is well-established in the literature for various metals, including gold, nickel, cobalt, copper, and palladium. The second step involves the formation of the Zn-based salen MOF framework followed by the incorporation of the reduced silver nanoparticles. Initially, zinc ions form helical complexes through adduct formation with

the organic nano-linker at the center skeleton. Subsequently, structural reordering occurs through the substrate binding of silver ions at the outer nodes of the complex, ultimately leading to the formation of the Ag@Zn-SalenMOF composite, in which silver nanoparticles are distributed throughout the MOF matrix.

1.1. Instrumentation and Characterization Techniques

The synthesized Ag@Zn-SalenMOF composite was characterized using a comprehensive array of analytical techniques to confirm its structure, morphology, and properties. Field emission scanning electron microscopy (FE-SEM) combined with energy-dispersive X-ray spectroscopy (EDX) was performed using a JEOL JSM-6510LV instrument (Japan) to investigate the surface morphology and elemental composition of the composite. The instrument was operated under standard conditions with appropriate acceleration voltages to obtain high-resolution images at various magnifications. High-resolution transmission electron microscopy (HR-TEM) analysis was conducted using a JEM-2100-JEOL instrument (Japan) with an acceleration voltage of up to 200 kV. This technique provided detailed information about the internal structure, particle size distribution, and crystallinity of the prepared composite. Selected area electron diffraction (SAED) patterns were also recorded to confirm the crystalline nature of the material. Fourier-transform infrared (FT-IR) spectroscopy was performed using a JASCO FT/IR-460 spectrophotometer (USA) to identify the functional groups and chemical bonds of the composite. Samples were prepared as KBr pellets, and spectra were recorded in the 400-4000 cm^{-1} range at room temperature with an appropriate resolution and scan numbers to achieve an optimal signal-to-noise ratio. UV-visible spectroscopy measurements were performed using a V-770 UV-Visible/NIR spectrophotometer (JASCO, USA) over a wavelength range of 200-2200 nm. The optical band gap was calculated using Optbandgap-204B software by applying the Tauc plot method to determine the electronic properties of the synthesized material. Fluorescence spectrum measurements were performed using FS5, Edinburgh instrument Co. UK.

Mass spectrometry analysis was performed using a Thermo Scientific ISQ single quadrupole mass spectrometer (USA) to determine the molecular weight and fragmentation pattern of the Ag@Zn-SalenMOF composite. The instrument was operated under appropriate ionization conditions to achieve optimal fragmentation and mass resolution.

Elemental analysis for carbon, hydrogen, and nitrogen content was determined using a Costech ECS-4010 analyzer (Italy). The instrument was calibrated with standard reference materials before analysis, and samples were combusted under controlled conditions to ensure accurate quantitative results. X-ray diffraction (XRD) analysis was performed using a D8-AVANCE X-ray diffractometer (Bruker, Germany) equipped with Cu-K α radiation ($\lambda = 0.154056 \text{ nm}$). The XRD patterns were recorded in the 2θ range from 3.0° to 80.0° with a step size of 0.020° and a scan speed of 0.4 seconds per step. This analysis provided information about the prepared composite's crystalline phase, relative crystallinity, and crystal size. X-ray photoelectron spectroscopy (XPS) measurements were conducted using a Thermo Scientific K-Alpha X-ray photoelectron spectrometer (USA) with an Al-K α micro-focused monochromator operating within an energy range up to 4 keV. This technique was employed to determine the oxidation states and chemical environment of different elements in the composite. ^1H -NMR spectroscopy was performed in DMSO- d_6 using a Gemini-300 MHz NMR spectrometer (ECA 500 II, JEOL, Japan) to confirm the structural integrity of the organic components within the composite.

framework. Thermogravimetric analysis (TGA) coupled with differential scanning calorimetry (DSC) was carried out using a Universal V4.5-TA instrument (USA) under atmospheric nitrogen gas flow with a heating rate of $10^{\circ}\text{C min}^{-1}$. This analysis provided information on the thermal stability, decomposition temperature, and thermal behavior of the synthesized composite. All data were analyzed using Origin-8 software for appropriate curve fitting and analysis.

3- Biosensor characterization:

3.1-Morphological Characterization and Surface Analysis

The field emission scanning electron microscopy (FE-SEM) analysis of the synthesized Ag@Zn-SalenMOF composite reveals distinctive morphological features that provide crucial insights into the hybrid material's structural organization and particle distribution. The comprehensive SEM investigation, conducted at multiple magnifications ranging from low to high resolution, demonstrates the successful formation of a well-defined nanocomposite structure with characteristic dual-phase morphology. The SEM micrographs in **Figure 1(a-e)** exhibit a heterogeneous surface morphology characterized by two distinct phases that can be differentiated based on their contrast and geometric features. The gray-colored regions observed throughout the images correspond to the Zn-MOF matrix, which forms the primary framework of the composite material. These regions display a characteristic slide-like morphology composed of aggregated nanosheets with well-defined square planar geometries. The dimensional analysis of these nanosheets reveals average dimensions of approximately 200×300 nm, indicating a relatively uniform size distribution within the MOF framework. The square planar morphology is consistent with the crystalline nature of the MOF structure. It suggests successful coordination of zinc ions with the organic salen linker, resulting in an ordered two-dimensional sheet-like arrangement. In stark contrast to the MOF matrix, the bright-colored regions visible in the SEM images represent the incorporated silver nanoparticles, which appear as highly dispersed aggregates distributed throughout the MOF matrix. The high-magnification FE-SEM analysis reveals that these silver nanoparticles exhibit a predominantly spherical morphology with remarkable monodispersity, indicating well-controlled nucleation and growth processes during the hydrothermal synthesis. The particle size analysis demonstrates that the silver nanoparticles possess diameters ranging from 150 to 200 nm, with an average diameter of approximately 189 nm, which correlates well with the subsequently obtained TEM results. The spherical morphology of the silver nanoparticles is attributed to the minimization of surface energy during the reduction process, where DMF acts as both a reducing agent and a stabilizing medium, preventing excessive aggregation and maintaining particle uniformity. The distribution pattern of silver nanoparticles within the MOF matrix appears to be highly homogeneous, with no evidence of significant phase separation or clustering. This uniform distribution is crucial for the composite's potential applications, as it ensures consistent properties throughout the material and maximizes the interfacial contact between the metallic nanoparticles and the MOF framework. The intimate contact between the silver nanoparticles and the MOF matrix suggests strong interfacial interactions, which may contribute to enhanced stability and synergistic effects in catalytic or sensing applications.

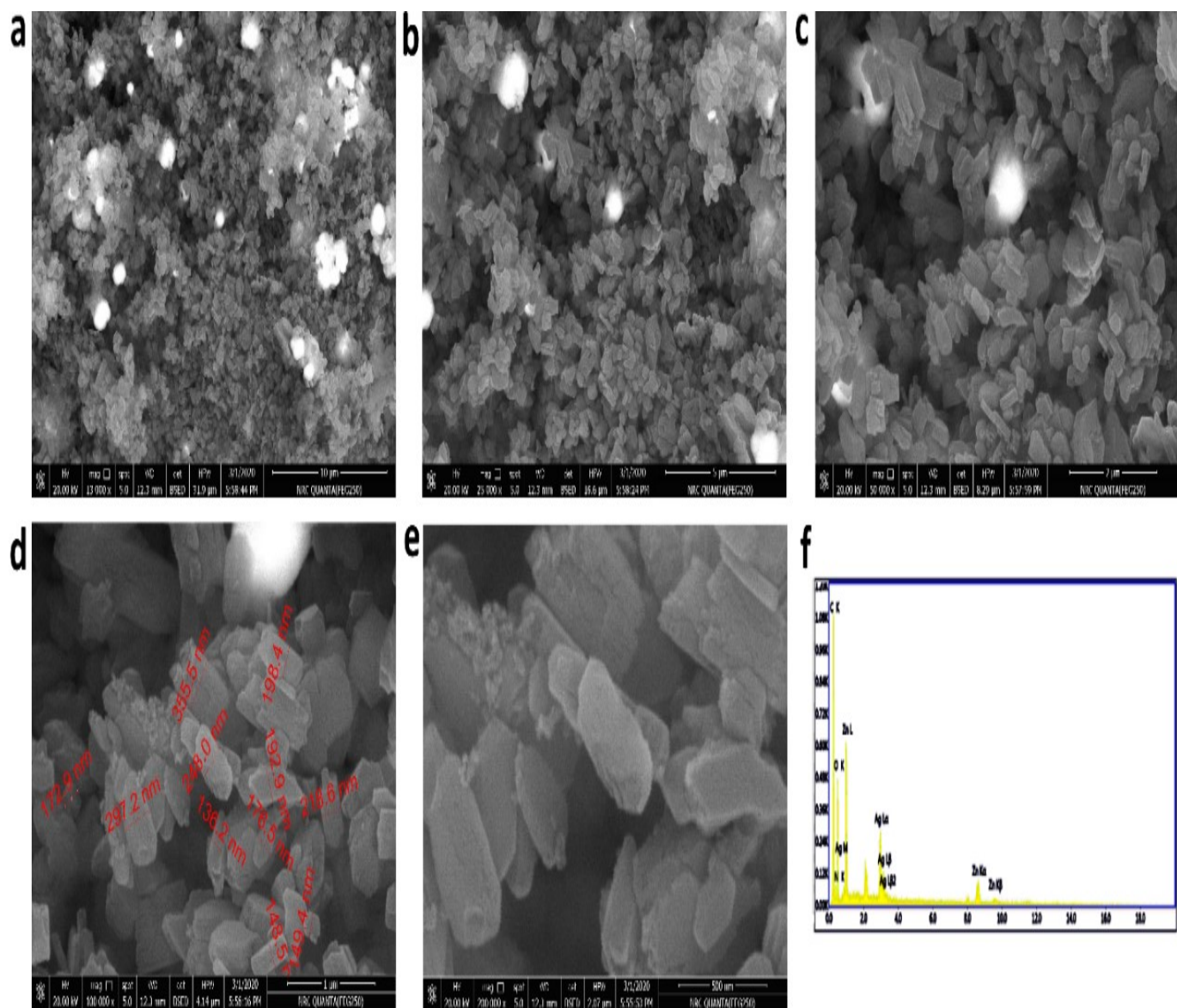


Figure S1. Field emission scanning electron microscopy analysis of Ag@Zn-SalenMOF composite: (a-d) SEM images at progressively increasing magnifications showing the overall morphology and particle distribution, (e) high-resolution SEM image revealing detailed surface features and particle size distribution, and (f) energy-dispersive X-ray (EDX) spectrum obtained from single-point analysis showing elemental composition.

The energy-dispersive X-ray (EDX) spectroscopy analysis provides quantitative elemental composition data and spatial distribution information for the Ag@Zn-SalenMOF composite. The EDX spectrum presented in **Figure S1(f)** identifies the presence of all expected elements: carbon (C), nitrogen (N), oxygen (O), zinc (Zn), and silver (Ag), confirming the successful incorporation of both metallic components within the organic framework structure. The absence of foreign elemental peaks in the spectrum indicates the high purity of the synthesized composite and the effectiveness of the purification procedures. The elemental mapping analysis presented in **Figure S2** provides crucial spatial distribution information that complements the quantitative data obtained from point analysis. **Figure S2(a)** displays the overlaid elemental mapping, demonstrating the homogeneous distribution of all constituent elements throughout the analyzed region. This overlay image is a composite representation of the elemental distribution, confirming that the silver nanoparticles are uniformly dispersed within the zinc-based MOF matrix without significant segregation or preferential accumulation in specific regions.

The individual elemental maps in **Figure S2(b-f)** provide detailed spatial information for each constituent element. The carbon and nitrogen maps reveal the uniform distribution of the organic salen linker throughout the framework, confirming the structural integrity of the MOF matrix. The oxygen distribution correlates well with the organic framework, comprising carboxylate and other oxygen-containing functional groups, as well as potentially coordinated water molecules. The zinc mapping delineates the MOF framework regions, showing a relatively uniform distribution corresponding to the gray areas observed in the SEM images. Most importantly, the silver mapping demonstrates that the metallic nanoparticles are distributed throughout the composite without forming large aggregates or clusters, which is essential for maintaining the composite's functional properties.

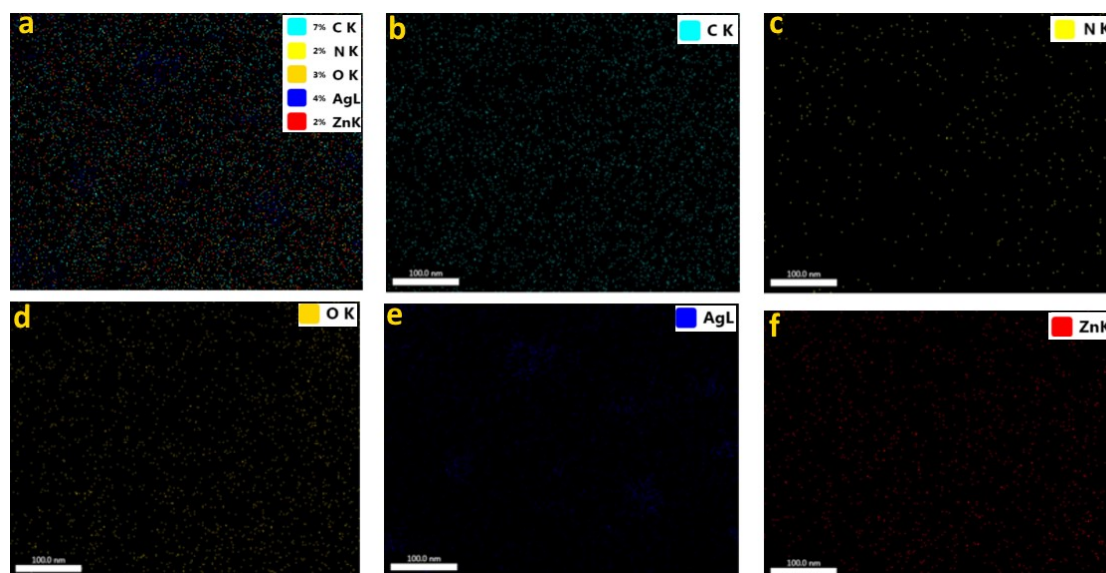


Figure S2. Energy-dispersive X-ray elemental mapping analysis of Ag@Zn-SalenMOF composite: (a) overlaid elemental map showing the combined distribution of all elements, (b) carbon distribution map, (c) nitrogen distribution map, (d) oxygen distribution map, (e) zinc distribution map, and (f) silver distribution map. The color-coded maps reveal the homogeneous distribution of elements throughout the composite structure.

The quantitative EDX analysis results in **Table 1** provide precise elemental composition data, which validate the proposed molecular formula and confirm the synthetic success. The weight percentages obtained experimentally show excellent agreement with the theoretical values calculated based on the proposed structure $C_{42}H_{41}Ag_2N_9O_{12}Zn_2$. The carbon content, determined to be 41.93 wt%, indicates successful incorporation of the organic salen linker without significant decomposition or loss during the hydrothermal synthesis. The silver content, measured at 18.34 wt%, confirms the successful reduction and incorporation of silver ions into the composite structure. This close agreement validates the proposed stoichiometry and suggests that the reduction mechanism proceeded efficiently under the reaction conditions employed. The slightly higher experimental value may be attributed to the formation of additional silver nanoparticles beyond the stoichiometric amount or surface-adsorbed silver species. The nitrogen content of 10.59 wt% confirms the presence of nitrogen-containing salen linkers and validates the structural integrity of the organic framework. The oxygen content, determined to be 17.91 wt%, can be attributed to the presence of coordinated or intercalated water molecules within the MOF framework, as commonly observed in hydrothermal synthesis products. The zinc content of 11.23 wt% confirms the successful incorporation of zinc ions into the MOF structure with the expected stoichiometry. The atomic percentages provided in **Table S1** offer additional insights into the elemental distribution. Carbon dominates the atomic composition at 41.93 wt%, reflecting the substantial organic content of the composite.

Table S1. Quantitative EDX elemental analysis of Ag@Zn-SalenMOF composite showing weight percentages, atomic percentages, net intensities, and measurement errors for all constituent elements.

Element	Weight %	Atomic %	Net Int.	Error %
C K	41.93	62.84	39.70	2.41
N K	10.59	12.69	2.64	11.62
O K	17.91	18.98	17.90	18.32
AgL	18.34	2.73	18.30	5.04
ZnK	11.23	2.76	10.10	3.01

3.2-Nanostructural Characterization and Crystallinity Assessment

The high-resolution transmission electron microscopy (HR-TEM) analysis provides unprecedented insight into the internal nanostructure and crystalline properties of the Ag@Zn-SalenMOF composite at the atomic scale. The TEM investigation, presented in **Figure 4(a-c)**, reveals the intimate structural details that complement and validate the surface morphology observations obtained from SEM analysis. The transmission electron microscopy technique offers superior resolution capabilities, enabling direct visualization of individual nanoparticles and their spatial arrangement within the MOF matrix.

The TEM micrographs demonstrate the presence of two distinct phases with markedly different electron density contrast. The regions exhibiting deep dark contrast correspond to the silver nanoparticles, which appear darker due to their higher atomic number and consequently higher electron scattering cross-section compared to the organic MOF framework. This contrast difference allows for precise identification and characterization of the metallic phase distribution within the composite structure. The silver nanoparticles exhibit a predominantly spherical morphology with remarkably uniform size distribution, confirming the SEM observations and validating the controlled nucleation and growth processes during synthesis.

Detailed particle size analysis from multiple TEM images reveals that the silver nanoparticles possess an average diameter of 189.0 nm, which shows excellent agreement with the SEM-derived measurements. The narrow size distribution indicates well-controlled synthetic conditions and effective stabilization by the MOF matrix, preventing excessive agglomeration during the hydrothermal treatment. The spherical morphology of the nanoparticles is consistent with thermodynamically favorable growth conditions where surface energy minimization drives the formation of isotropic particles. The MOF framework appears as lighter contrast regions surrounding and encapsulating the silver nanoparticles, forming small nano-slides or nanosheets as observed in the SEM analysis. The TEM images reveal that these MOF nanosheets maintain their structural integrity even at the nanoscale, indicating robust framework stability under the synthesis conditions. The intimate contact between the silver nanoparticles and the MOF matrix suggests strong interfacial interactions, crucial for charge transfer processes and synergistic effects in potential applications. The selected area electron diffraction (SAED) pattern presented in **Figure S3(d)** provides critical information about the crystalline nature of both phases within the composite. The SAED pattern exhibits distinct diffraction rings and spots, confirming the polycrystalline nature of the material. The presence of ring patterns and discrete spots indicates the coexistence of randomly oriented crystalline domains (contributing to ring patterns) and larger single-crystalline regions (contributing to discrete spots). This diffraction pattern validates the crystalline nature of the silver nanoparticles and the Zn-MOF nanosheets, confirming the successful formation of crystals during hydrothermal synthesis. The ring patterns in the SAED can be attributed to the polycrystalline silver nanoparticles, where multiple small crystallites contribute to the diffraction

pattern. The discrete spots likely originate from larger MOF crystalline domains that are favorably oriented concerning the electron beam. Combining these diffraction features confirms the successful formation of a crystalline nanocomposite where both phases maintain their crystalline integrity while forming an integrated hybrid structure.

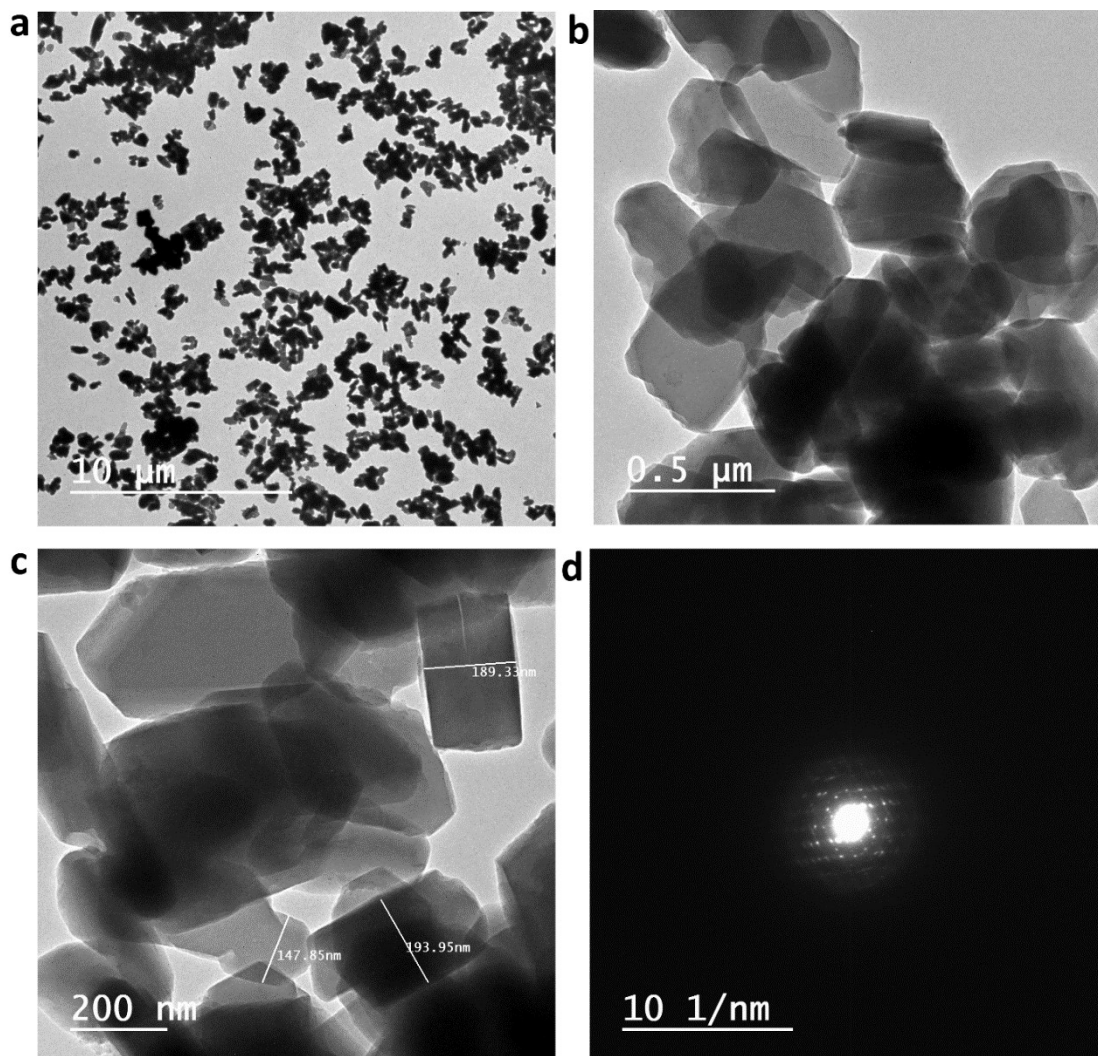


Figure S3. High-resolution transmission electron microscopy analysis of Ag@Zn-SalenMOF composite: (a-c) TEM images at different magnifications showing the internal nanostructure, particle distribution, and size uniformity of silver nanoparticles within the MOF matrix, and (d) selected area electron diffraction (SAED) pattern confirming the polycrystalline nature of both silver nanoparticles and MOF nanosheets.

3.3- X-ray Photoelectron Spectroscopy Analysis

The X-ray photoelectron spectroscopy (XPS) analysis provides comprehensive information about the surface chemical composition, oxidation states, and electronic environment of elements within the Ag@Zn-SalenMOF composite. This surface-sensitive technique offers crucial insights into the chemical bonding, coordination environment, and electronic interactions between different components of the hybrid material. The XPS investigation validates the successful incorporation of all constituent elements and confirms their expected chemical states. The XPS broad scan survey spectrum, presented in Figure 5(a), demonstrates the presence of all elements, without any detectable impurities, confirming the high purity of the synthesized composite. The survey spectrum clearly shows characteristic

photoelectron peaks for carbon (C 1s at ~285 eV), oxygen (O 1s at ~532 eV), nitrogen (N 1s at ~401 eV), zinc (Zn 2p at ~1022 and ~1045 eV), and silver (Ag 3d at ~368 and ~374 eV). The absence of any foreign element peaks validates the effectiveness of the purification procedures and confirms that the synthesis proceeded without contamination from side products or unreacted precursors. The quantitative analysis from the survey scan reveals a significant surface enrichment of carbon (72.79 atomic%), which is expected given the organic nature of the salen linker framework. The nitrogen content (13.52 atomic percent) confirms the presence of a nitrogen-containing organic linker, while the oxygen content (11.54 atomic percent) corresponds to various oxygen-containing functional groups within the framework. The metallic components exhibit lower surface concentrations, with zinc at 1.75 atomic percent and silver at 0.41 atomic percent, indicating that these elements are primarily incorporated within the framework structure rather than enriched at the surface.

The high-resolution Zn 2p spectrum shown in **Figure S4(b)** exhibits the characteristic spin-orbit doublet with peaks at 1021.87 eV (Zn 2p_{3/2}) and 1044.90 eV (Zn 2p_{1/2}), corresponding to a spin-orbit coupling of approximately 23.03 eV. These binding energies are consistent with Zn²⁺ oxidation state in a coordination environment typical of MOF structures. The deconvolution analysis reveals multiple components within each peak, suggesting different coordination environments for zinc atoms within the framework. The primary components at 1021.87 eV and 1044.90 eV (38.38% and 31.26% of the total Zn 2p signal, respectively) correspond to zinc atoms coordinated to the organic salen linker in the main framework structure. Additional minor components were observed at 1039.97 eV, 1022.02 eV, and 1047.66 eV, contributing 9%, 20.32%, and 1.05%, respectively. These observations suggest the presence of zinc atoms in slightly different coordination environments, possibly including surface species, defect sites, or zinc atoms with varying degrees of coordination saturation. This multiplicity of zinc environments is common in MOF structures and reflects the complexity of the three-dimensional framework architecture.

The O 1s spectrum presented in **Figure 5(c)** shows three distinct components after deconvolution, located at 530.72 eV, 531.07 eV, and 532.37 eV, with relative contributions of 27.05%, 44.43%, and 28.52%, respectively. The component at 530.72 eV can be attributed to oxygen atoms in metal-oxygen bonds (M-O), specifically zinc-oxygen coordination bonds within the MOF framework. The peak at 531.07 eV corresponds to oxygen atoms in organic functional groups, particularly C=O bonds in carboxylate groups of the salen linker. The highest binding energy component at 532.37 eV is characteristic of C-O bonds in organic moieties and potentially physisorbed water molecules or hydroxyl groups on the surface. The N 1s spectrum shown in **Figure S4(d)** exhibits a single, symmetric peak centered at 400.94 eV, indicating a uniform nitrogen environment within the composite. This binding energy is characteristic of nitrogen atoms in aromatic amine environments, specifically the nitrogen atoms in the salen ligand coordinated to zinc centers. A single, well-defined peak suggests that all nitrogen atoms exist in similar chemical environments, confirming the structural uniformity of the organic linker coordination. The Ag 3d high-resolution spectrum presented in **Figure 5(e)** displays the characteristic spin-orbit doublet with peaks at 367.99 eV (Ag 3d_{5/2}) and 373.95 eV (Ag 3d_{3/2}), corresponding to a spin-orbit splitting of 5.96 eV. These binding energies are consistent with metallic silver (Ag⁰), confirming the successful reduction of silver ions during the synthesis process. The deconvolution analysis reveals that the primary components, accounting for 29.37% and 37.28% of the total signal, correspond to metallic silver nanoparticles. Minor components at 368.19 eV and 375.44 eV (31.77% and 1.58% respectively) may indicate the presence of surface-oxidized silver species or silver atoms in different coordination environments at the nanoparticle-MOF interface. The C 1s spectrum shown in **Figure S4(f)** exhibits three distinct components after deconvolution, reflecting the diverse carbon environments within the organic framework. The main component at 284.48 eV (74.13% of the total signal) corresponds to the aromatic and aliphatic C-C and C-H bonds of the organic linker backbone. The component at 285.77 eV (17.31%) is attributed to C-N bonds, confirming the nitrogen-carbon connectivity in the salen ligand structure. The highest binding energy component at 287.93 eV

(8.56%) corresponds to C=O bonds in carboxylate functional groups, validating the presence of the carboxylic acid functionality essential for MOF formation.

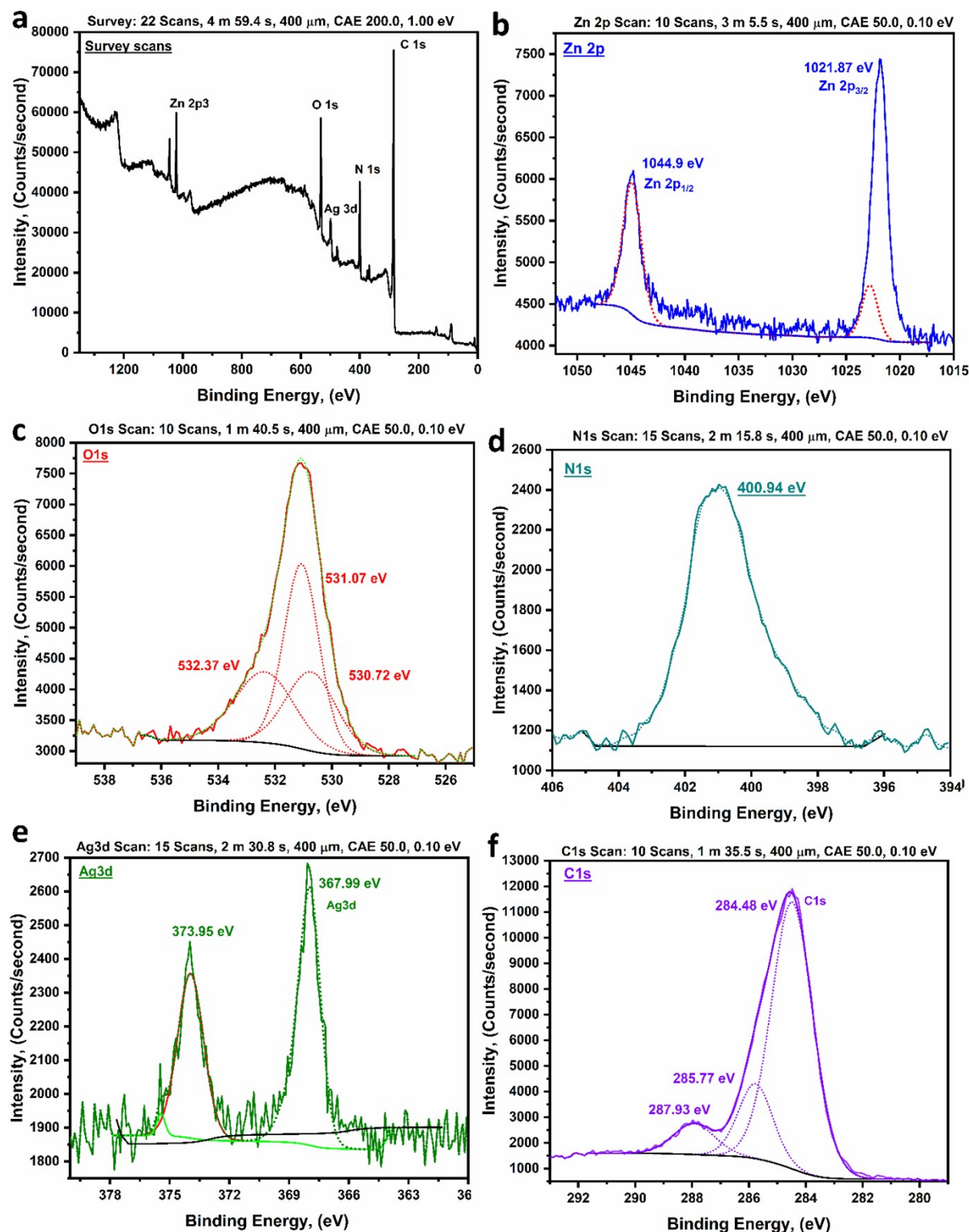


Figure S4. X-ray photoelectron spectroscopy analysis of Ag@Zn-SalenMOF composite: (a) XPS survey spectrum showing all constituent elements without impurities, (b) high-resolution Zn 2p spectrum with deconvolution showing multiple zinc coordination environments, (c) high-resolution O 1s spectrum revealing different oxygen bonding states, (d) high-resolution N 1s spectrum showing uniform nitrogen environment, (e) high-resolution Ag 3d spectrum confirming metallic silver

formation, and (f) high-resolution C 1s spectrum displaying various carbon bonding environments within the organic framework. The comprehensive XPS analysis confirms the successful synthesis of the Ag@Zn-SalenMOF composite with all elements present in their expected oxidation states and coordination environments. The data validate the proposed structure, where zinc atoms coordinate to the organic salen linker to form the MOF framework, while silver exists predominantly as metallic nanoparticles distributed throughout the structure. The surface chemical analysis supports the mechanism of DMF-mediated silver reduction and subsequent incorporation into the MOF matrix, providing definitive evidence for the successful formation of the targeted hybrid nanocomposite.

3.4- X-ray Diffraction (XRD) Analysis

The X-ray diffraction analysis presented in Figure 6 provides crucial crystallographic evidence for the successful synthesis and structural integrity of the Ag@Zn-SalenMOF composite material. The diffractogram reveals a series of well-defined, sharp diffraction peaks that collectively demonstrate the highly crystalline nature of the synthesized composite, confirming the ordered arrangement of atoms within the crystal lattice structure. The diffraction pattern exhibits characteristic peaks at specific 2θ values: 7.29° , 11.13° , 13.69° , 17.35° , 20.18° , 21.99° , 22.96° , 26.7° , 27.63° , 29.11° , 38.15° , 44.56° , 64.78° , and 77.54° . These peak positions are particularly significant, corresponding to specific crystallographic planes and interplanar spacings within the composite structure. The presence of peaks at low 2θ values (7.29° and 11.13°) is characteristic of metal-organic framework materials, indicating the formation of extended periodic structures with relatively large unit cell parameters, consistent with the incorporation of bulky organic salen linkers. The diffraction data has been systematically compared with standard reference patterns, specifically JCPDS card no. 18-1486 for Zn-MOF and JCPDS card no. 87-0720 for metallic silver. This comparison provides definitive evidence for the coexistence of both zinc-based MOF framework and silver nanoparticles within the composite structure. The match with these reference patterns confirms the dual-phase nature of the material, where silver nanoparticles are successfully incorporated into the zinc-salen MOF matrix. The sharpness and intensity of the observed peaks indicate good crystallinity and relatively large crystallite sizes, suggesting that the hydrothermal synthesis conditions (200°C for 8 hours) were optimal for achieving well-ordered crystal growth. The absence of peak broadening or amorphous backgrounds further supports the high degree of structural order within the composite. Additionally, the XRD results corroborate the findings of the transmission electron microscopy (TEM) analysis, providing complementary evidence for the crystalline nature of the MOF framework and the embedded silver nanoparticles.

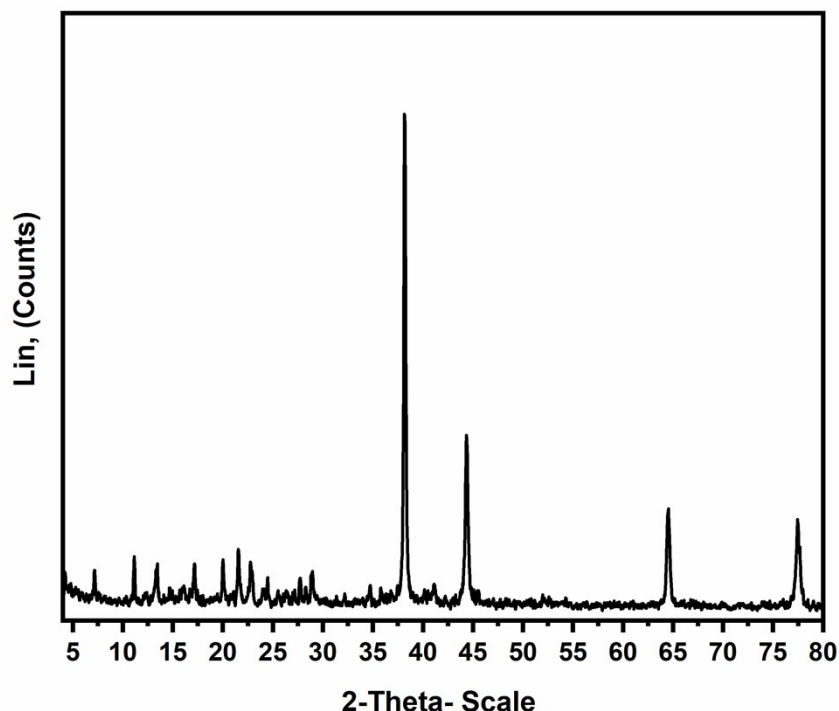


Fig. S5: The X-ray diffraction spectra of Ag@Zn-SalenMOF.

3.5-Mass Spectrum of Ag@Zn-SalenMOF

The mass spectrometry analysis presented in **Figure 7** provides detailed molecular-level information about the composition and fragmentation behavior of the Ag@Zn-SalenMOF composite. The mass spectrum reveals the molecular ion peak and subsequent fragmentation pattern, which serves as a molecular fingerprint for structural confirmation and compositional analysis. The most significant feature of the mass spectrum is the molecular ion peak observed at $m/z = 1028.12 \text{ g mol}^{-1}$, which corresponds to the intact Ag@Zn-SalenMOF composite after the loss of two water molecules and two N,N-dimethylformamide (DMF) molecules during the ionization process. This experimental value shows excellent agreement with the theoretical molecular weight calculation, providing strong evidence in support of the proposed molecular structure. The loss of solvent molecules (H_2O and DMF) is commonly observed in mass spectrometry of MOF materials due to their relatively weak coordination compared to the primary framework bonds.

The spectrum also displays a series of characteristic fragment ions at m/z values of 759.78, 488.20, 272.31, 164.01, 148.30, 108.02, 181.04, and 64.95 g mol^{-1} . These fragmentation peaks provide valuable structural information about the decomposition pathways of the organic salen linker backbone. The close correspondence between experimental and theoretical fragmentation values (758.13, 488.13, 272.01, 165.15, 149.15, 108.14, 181.19, and 65.38 g mol^{-1} respectively) validates the proposed molecular structure and confirms the identity of the synthesized composite. The fragmentation pattern follows a logical sequence that reflects the inherent stability of different molecular segments within the composite structure. The larger fragments (759.78 and 488.20 g mol^{-1}) likely correspond to partial decomposition of the organic framework. In comparison, smaller fragments represent individual organic moieties or metal-ligand complexes that retain structural integrity during ionization.

Sheta-2 #751 RT: 2.58 AV: 1 NL: 6.41E6
T: {0,0} + c EI Full ms [50.00-1100.00]

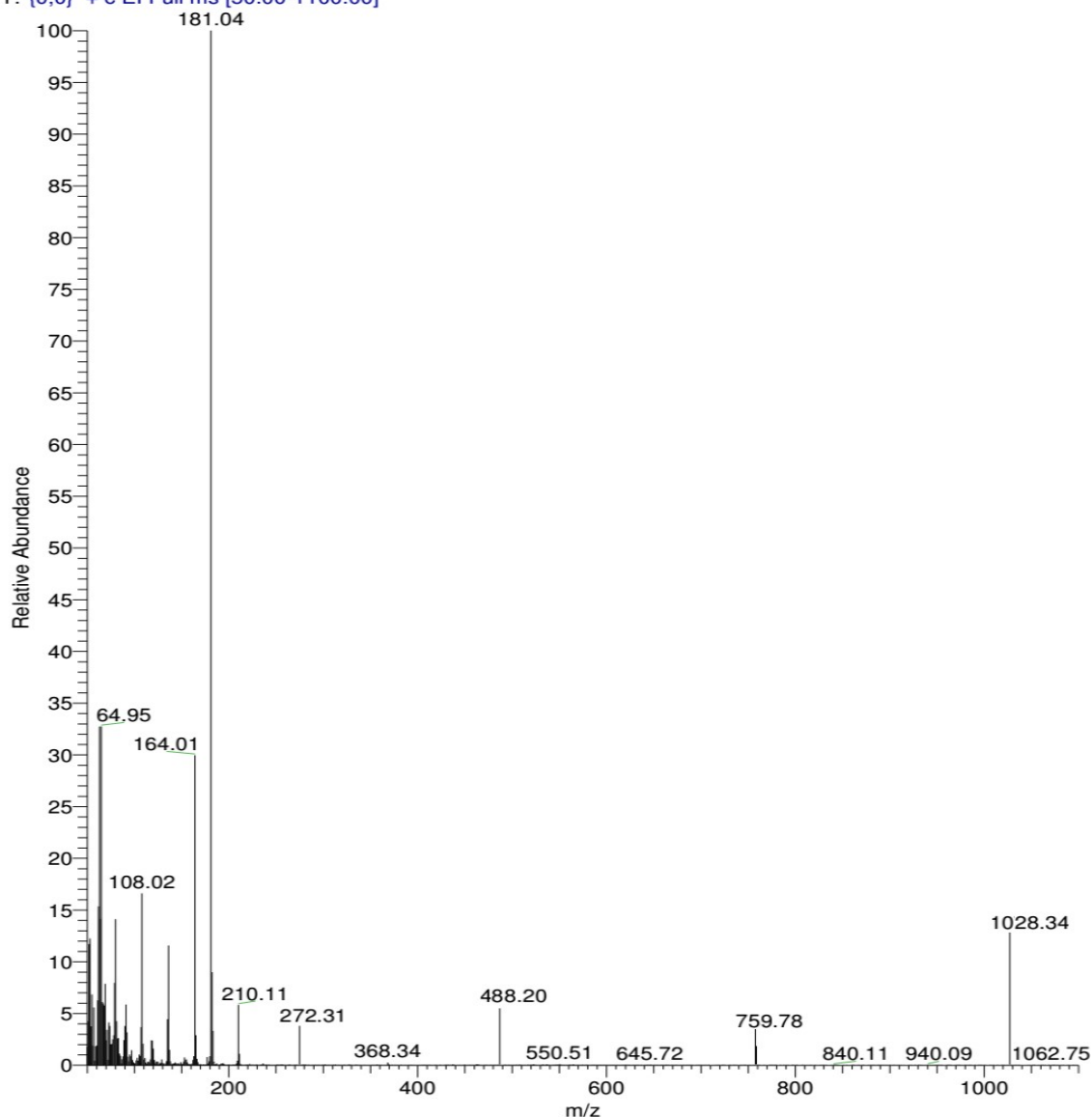


Fig. S6: The mass spectrum of the Ag@Zn-SalenMOF .

3.6-Proposed Fragmentation Scheme of Ag@Zn-SalenMOF

Figure 8 presents a comprehensive fragmentation scheme that illustrates the systematic breakdown pathway of the Ag@Zn-SalenMOF composite under mass spectrometric conditions. This fragmentation map is a roadmap for understanding the structural stability and decomposition behavior of different molecular components within the composite.

The fragmentation scheme begins with the molecular ion of the intact composite and proceeds through a series of logical bond cleavages that reflect the relative bond strengths within the molecule. The initial fragmentation typically involves the loss of weakly coordinated solvent molecules (water and DMF), followed by more extensive decomposition of the organic salen framework. The scheme demonstrates how different structural elements of the composite exhibit varying degrees of stability under ionization conditions. Each fragmentation step is characterized by specific mass losses corresponding to identifiable molecular fragments, such as aromatic rings, aliphatic chains, or metal-ligand coordination complexes. The proposed pathways are consistent with known fragmentation patterns of similar salen-

based metal complexes and MOF materials, providing additional validation for the structural assignment.

The fragmentation analysis reveals essential information about the metal centers' coordination environment and the MOF framework's connectivity patterns. Observing specific fragment ions containing zinc and silver suggests intimate mixing of these metals within the composite structure, rather than simple physical mixing of separate phases. This supports the proposed mechanism of silver incorporation into the zinc-salen MOF matrix through substrate binding at outer coordination sites. The mass spectrometric data, when combined with the fragmentation scheme, provides compelling evidence for the successful synthesis of the targeted Ag@Zn-SalenMOF composite with the proposed molecular structure. The excellent agreement between experimental and theoretical fragmentation patterns confirms both the composition and structural integrity of the synthesized material, supporting the overall characterization results obtained from other analytical techniques.

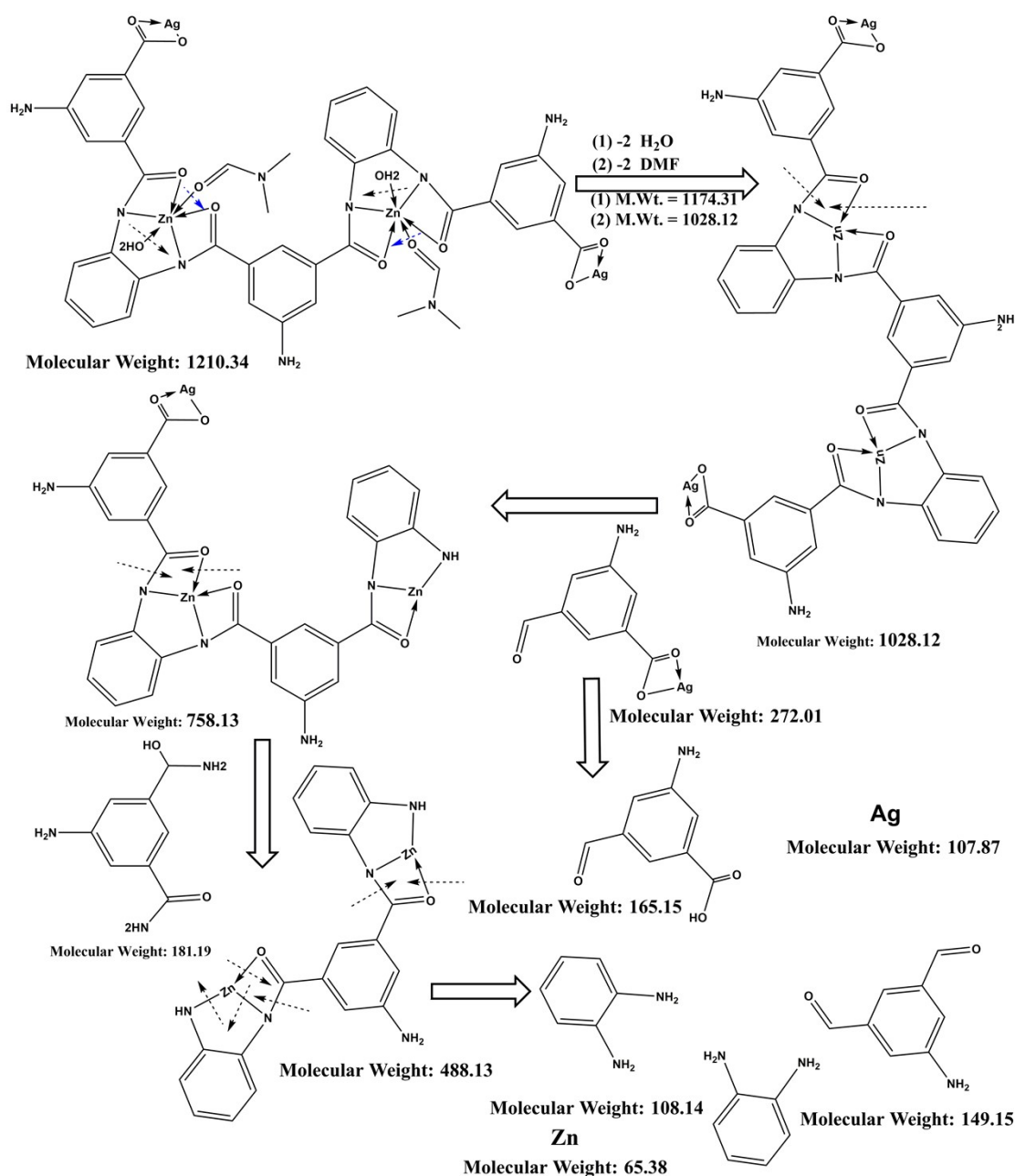


Fig. S7: The proposed fragmentation scheme of the Ag@Zn-SalenMOF.

3.7- UV-Visible Spectroscopy Analysis

The UV-visible absorption spectrum presented in **Figure S8** provides crucial information about the electronic structure and optical properties of the Ag@Zn-SalenMOF composite. The spectrum reveals four distinct absorption peaks at 234, 288, 347, and 626 nm, each corresponding to specific electronic transitions within the composite material. These absorption features represent a complex interplay between the electronic states of the organic salen ligands, zinc metal centers, and incorporated silver nanoparticles.

The absorption peak at 234 nm is attributed to high-energy $\pi \rightarrow \pi^*$ transitions within the aromatic rings of the salen ligand framework. This transition represents the promotion of electrons from bonding π orbitals to antibonding π^* orbitals in the conjugated aromatic system. The relatively high intensity of this peak indicates extensive π -conjugation within the organic framework, which is characteristic of salen-based ligand systems. The absorption at 288 nm corresponds to charge transfer transitions, likely involving metal-to-ligand charge transfer (MLCT) processes between the zinc centers and the salen ligands. This transition is particularly significant as it reflects the electronic coupling between the metal centers and the organic framework, confirming the successful coordination of zinc ions within the MOF structure. The peak at 347 nm is associated with lower energy $\pi \rightarrow \pi^*$ transitions within the extended conjugated system of the composite. The red-shift of this transition compared to free salen ligands indicates increased conjugation and electronic delocalization upon MOF formation. This is consistent with the framework structure where multiple salen units are interconnected through metal nodes. The broad absorption feature at 626 nm is particularly noteworthy as it extends into the visible region and is characteristic of surface plasmon resonance (SPR) effects associated with the silver nanoparticles embedded within the MOF matrix. This more extended wavelength absorption confirms the presence of metallic silver nanoparticles. It suggests their successful incorporation into the composite structure without significant aggregation, as excessive aggregation would typically result in further red-shifting and broadening of the SPR band. The observed considerable blue-shift compared to the free organic linker indicates strong electronic interactions between the different components of the composite. This blue-shift phenomenon suggests that the electronic environment of the organic chromophores has been significantly altered upon incorporation into the MOF structure and subsequent inclusion of silver nanoparticles.

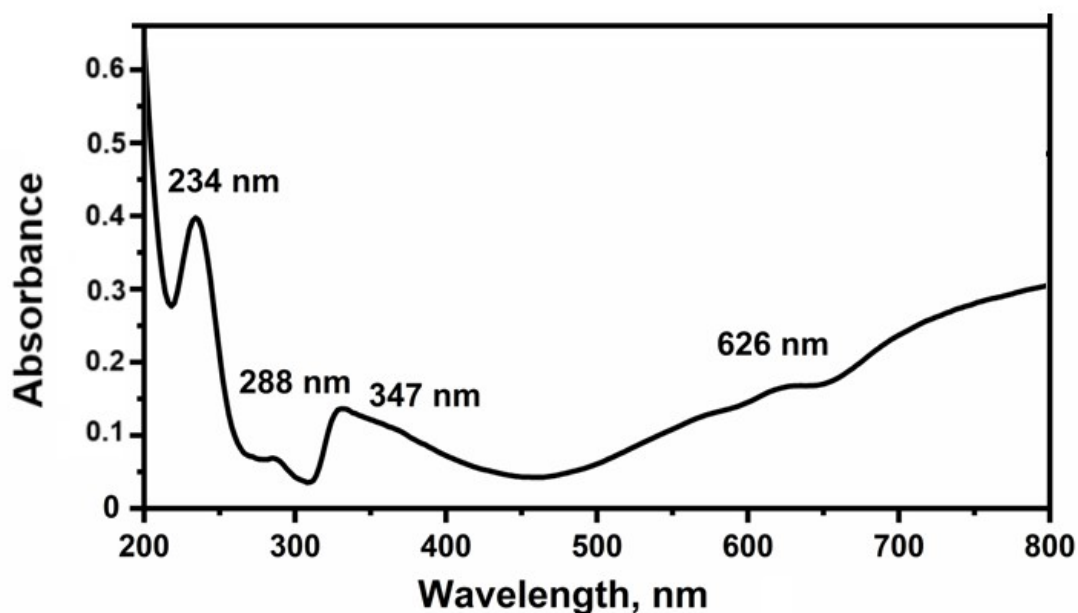


Fig. S8: The electronic absorption spectra of Ag@Zn-SalenMOF .

3.8-Band Gap Energy Analysis of Ag@Zn-SalenMOF

Figure S9 presents the Tauc plot analysis used to determine the optical band gap energies of the Ag@Zn-SalenMOF composite. The study reveals three distinct band gap values at 1.17, 1.61, and 1.87 eV, indicating the presence of multiple electronic transitions and energy levels within the composite material. These multiple band gaps are characteristic of complex heterogeneous materials where different phases and interfaces contribute to the overall electronic structure. The presence of numerous band gaps reflects the hierarchical electronic structure of the composite, where each component—zinc-salen MOF framework, silver nanoparticles, and interfacial regions—contributes distinct electronic states. The lowest band gap value of 1.17 eV corresponds to the narrowest energy separation between occupied and unoccupied electronic states, likely associated with charge transfer processes between the silver nanoparticles and the MOF framework. This relatively small band gap suggests potential semiconducting properties and possible applications in photocatalytic processes. The intermediate band gap of 1.61 eV is attributed to electronic transitions within the zinc-salen MOF framework, representing the energy required for electron promotion from the highest occupied molecular orbital (HOMO) to the lowest unoccupied molecular orbital (LUMO) of the coordinated salen ligands. This value is consistent with typical band gaps observed in similar MOF materials and indicates suitable electronic properties for various applications. The highest band gap of 1.87 eV likely corresponds to transitions within the pure organic salen framework, representing the intrinsic electronic properties of the ligand system. The reduction in band gap values compared to the free organic linker is attributed to the increased conjugation and electronic delocalization upon MOF formation and metal coordination. The significant decrease in band gap energies compared to the corresponding values in the free linker results from the enhanced conjugation of the ligand system due to coordination with metal centers. This electronic modification results in an increase in the energy of the HOMO (valence band), effectively narrowing the HOMO-LUMO gap and facilitating more accessible electronic transitions. This band gap engineering, achieved through metal coordination and nanoparticle incorporation, is highly desirable for developing materials with tailored electronic and optical properties.

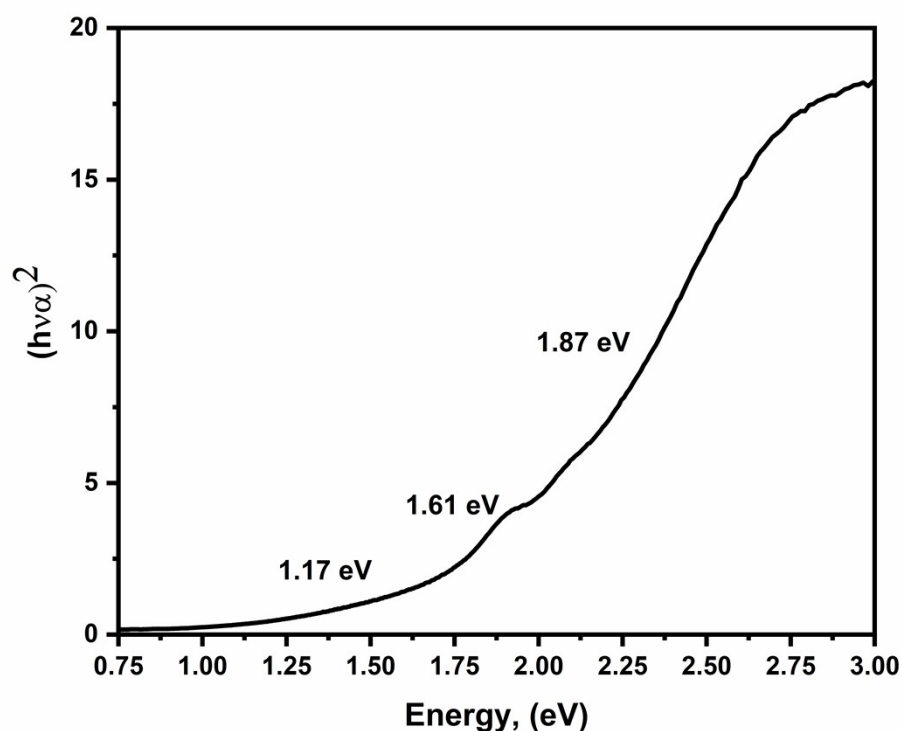


Fig. S9: The band gap energy of Ag@Zn-SalenMOF.

3.9- Thermogravimetric Analysis

The thermogravimetric analysis (TGA) presented in **Figure S10** provides comprehensive information about the thermal stability and decomposition behavior of the Ag@Zn-SalenMOF composite. The thermogram reveals a multi-stage decomposition process that reflects the hierarchical structure of the composite material, with different components exhibiting distinct thermal stabilities. The first stage of weight loss occurs between 26.78°C and 178.57°C, corresponding to a 2.97% reduction in weight. This initial weight loss is attributed to the removal of physisorbed and inter-lattice water molecules that are weakly bound within the MOF pores and crystal lattice. The relatively low temperature range for this process confirms that these water molecules are not strongly coordinated to the metal centers but rather exist as guest molecules within the framework cavities. The second decomposition stage spans from 178.57°C to 334.21°C, resulting in a more significant weight loss of 12.43%. This stage corresponds to the elimination of DMF (N,N-dimethylformamide) molecules that were incorporated during the synthesis process.

The higher temperature required for DMF removal compared to water indicates stronger interactions with the framework, possibly through coordination to metal centers or hydrogen bonding with the organic ligands. The complete removal of DMF at this temperature range confirms the successful activation of the MOF structure. The major decomposition event begins at 334.21°C and continues to higher temperatures, accounting for a substantial 44.78% weight loss. This stage represents the breakdown of the organic salen framework, including the decomposition of aromatic rings, aliphatic linkers, and coordination bonds between the organic ligands and metal centers. The onset temperature of 334°C indicates excellent thermal stability of the MOF framework, which is crucial for practical applications requiring elevated temperature operation. The composite demonstrates remarkable thermal stability, maintaining structural integrity up to approximately 340°C before significant decomposition begins. The broad temperature range for framework decomposition (340-995°C) suggests a gradual

breakdown process rather than catastrophic failure, indicating robust intermolecular interactions and strong metal-ligand coordination bonds within the structure. After heating to 994.95°C, the remaining residue accounts for 39.87% of the original weight, corresponding to the metallic components (silver and zinc) that remain after complete organic framework decomposition. This residual weight percentage is in excellent agreement with the theoretical metal content calculated from the proposed molecular formula, providing additional validation for the structural assignment and composition of the composite. The TGA results demonstrate exceptional agreement with both the mass spectrometry fragmentation data and XRD crystallographic analysis, creating a consistent picture of the composite's structure and composition. The thermal stability profile positions this material as suitable for applications requiring moderate to high temperature operation while maintaining structural integrity.

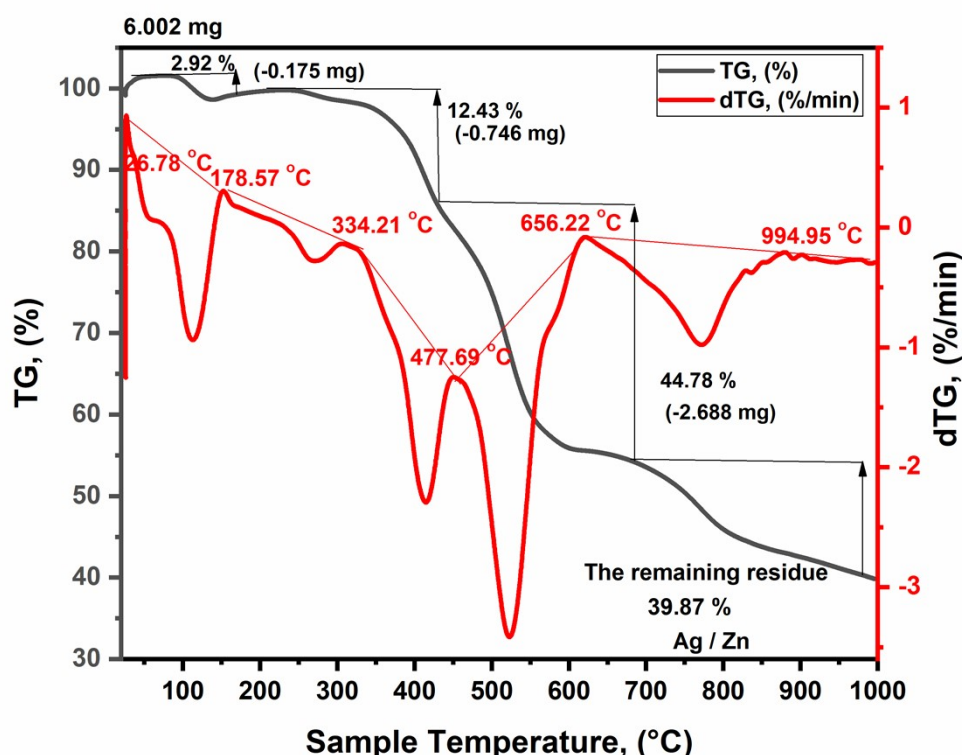


Fig. S10: The thermogravimetric analysis of the Ag@Zn-SalenMOF.

3.10-Proposed Molecular Structure

Figure S11 presents the comprehensive three-dimensional molecular structure of the Ag@Zn-SalenMOF composite, integrating all characterization data to provide a unified structural model. This proposed structure represents the culmination of extensive analytical evidence and provides insight into the spatial arrangement of atoms, coordination environments, and overall architecture of the composite material. The structure reveals a sophisticated hierarchical organization where zinc metal centers serve as primary nodes connecting the organic salen ligands into an extended three-dimensional framework. Each zinc center adopts a coordination geometry consistent with the spectroscopic evidence, likely involving coordination to nitrogen and oxygen atoms from multiple salen ligands. This coordination pattern establishes the fundamental MOF architecture, characterized by well-defined pores and channels that are typical of metal-organic framework materials.

The silver nanoparticles are strategically positioned within the MOF matrix, as evidenced by the microscopic and spectroscopic analyses. Rather than existing as isolated entities, the silver components

appear to be intimately integrated into the framework structure, possibly through coordination to peripheral sites on the salen ligands or interaction with the zinc coordination spheres. This intimate integration explains the unique electronic and optical properties observed in the UV-visible spectroscopy analysis. The proposed structure accounts for the observed stoichiometry of $C_{42}H_{41}Ag_2N_9O_{12}Zn_2$ with a molecular weight of 1210.34 g/mol, which corresponds perfectly with the elemental analysis and mass spectrometry results. The arrangement illustrates how two zinc centers and two silver atoms are incorporated into a framework comprising nine nitrogen atoms and twelve oxygen atoms, consistent with the coordination requirements of the salen ligand system. The three-dimensional architecture explains the observed porosity and surface area characteristics, as well as the thermal stability profile demonstrated in the TGA analysis. The framework design incorporates microporous and mesoporous regions, created by the intersection of organic linkers and the spatial arrangement of metal nodes. These porous regions are crucial for potential applications in catalysis, gas storage, or sensing. The structural model also rationalizes the observed electronic properties, particularly the multiple band gaps and charge transfer processes identified in the optical characterization. The intimate contact between silver nanoparticles and the zinc-salen framework creates unique interfacial electronic states that contribute to the overall electronic structure and enable efficient charge transfer processes. This comprehensive structural proposal, supported by multiple analytical techniques, establishes a solid foundation for understanding the relationship between structure and properties in the Ag@Zn-SalenMOF composite, enabling rational design of similar materials with tailored characteristics for specific applications.

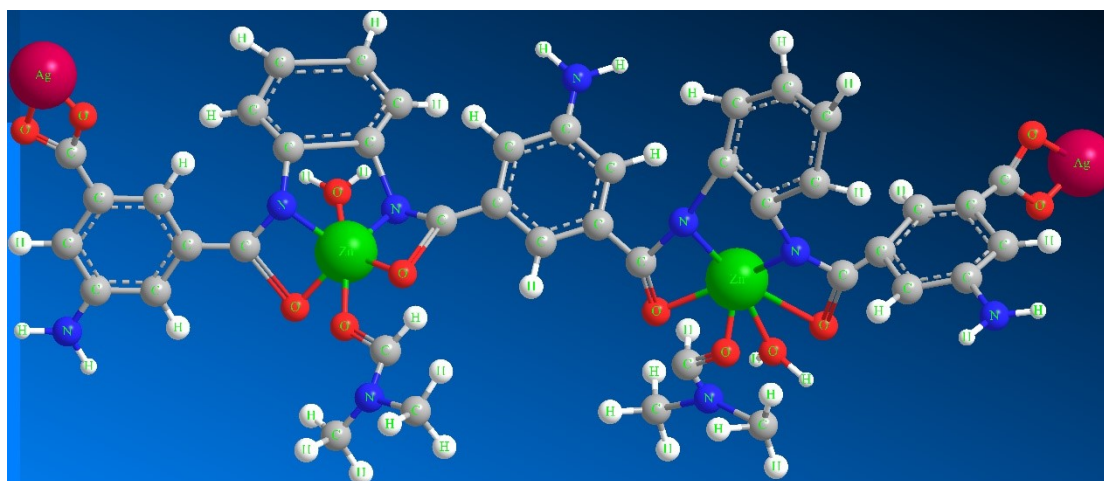


Fig. S11: The proposed structure of the Ag@Zn-SalenMOF .